Continuous wave dual-wavelength Nd:YVO_4 laser working at 1064 and 1066 nm

Shuaijun Zhou (周帅军), Peng Gu (谷 鹏), Xiaoli Li (李小丽)*, and Shibing Liu (刘世炳)

Institute of Laser Engineering, Beijing University of Technology, Beijing 100124, China
**Corresponding author: lilyli@bjut.edu.cn*

Received January 20, 2017; accepted March 24, 2017; posted online April 10, 2017

We demonstrate a continuous-wave (CW) dual-wavelength Nd:YVO_4 laser working at 1064 and 1066 nm simultaneously. The method of Nd:YVO_4 crystal angle tuning is used to balance the ratio of the stimulated emission cross sections of the two wavelengths, leading to the realization of a simultaneous dual-wavelength operation from only one laser. The experimental results show that at a 2.85 W pump power, the maximum output powers at wavelengths of 1064 and 1066 nm are 0.55 and 0.54 W, respectively. The linear resonate cavity is as short as 10 mm, which gives the laser the advantages of a miniature configuration and low threshold. Such a dual-wavelength laser can be very attractive for the development of compact THz sources based on difference frequency generation.

OCIS codes: 140.3580, 1403615, 1403600.
doi: 10.3788/COL201715.071401.

The generation of terahertz (THz) radiation has gained rising interest due to its potential to be widely used in medicine, biology, homeland security, and other applications[1–4]. However, the uptake of THz technologies is hampered by a lack of powerful and cost-effective sources. In the past decade, there has been a large amount of activities focusing on the development of compact THz laser sources. One of the most practical and efficient methods is based on optical frequency mixing within conventional Nd lasers. The employed nonlinear conversion processes include difference frequency generation (DFG), optical parametric oscillation (OPO), and stimulated polariton scattering (SPS)[1,3,5]. In this Letter, we are concerned with simultaneous dual-wavelength operation in an Nd laser used for the DFG method.

To reach simultaneous dual-wavelength emission from only one Nd laser, three main frequency controlling routes have been utilized. The first one stimulates two transitions from different energy levels in a laser crystal to generate dual-wavelength emissions with a relatively large frequency separation on the scale of 10 THz, such as 1.06 and 1.3 μm[6]. The second one focuses on one transition with Stark splitting of involved energy levels, which can generate dual-wavelength emissions with a relatively small frequency separation on the scale of 0.1 THz, such as 1063 and 1066 nm[7]. The third one stimulates a fundamental wavelength and then shifts it to another wavelength by some nonlinear process, such as stimulated Raman scattering[8] and SPS[1,3], which can generate dual-wavelength emission with a several THz frequency separation. In 2011, Sirotkin *et al.*[9] reported continuous-wave (CW) tuning of a *c*-cut Nd:YVO_4 laser from 1062 to 1067 nm, and radiation at 1062 and 1066 nm was also obtained. Zhao *et al.*[10] reported a THz source with orthogonal linearly polarized lasers at 1047 and 1053 nm by using an Nd:YLF crystal as the active gain medium. In 2013, control of laser emissions by selecting crystal orientations was used to get emission wavelengths in the range of 1061 to 1068 nm[11]. Reference [12] realized an Nd:YLF laser at a cryogenic temperature with orthogonally polarized simultaneous emission at 1047 and 1053 nm. More recently, Brenier[13] equalized the emission cross sections at 1047 and 1053 nm by adjusting the propagation direction out of the principal axes. Lin *et al.*[14] employed a simple glass etalon to modulate the intra-cavity losses to achieve multi-wavelength linearly polarized Nd:YVO_4 lasers at 1062, 1064, and 1066 nm. According to the reported experimental results[15–19], the stability of the output power and the conversion efficiency of the above dual-wavelength lasers need to be improved by a special cavity design, advanced mirror coating, or by using additional optical elements, such as an intracavity etalon and a polarization beam splitter. Those with orthogonal linearly polarized laser[9–14] outputs could be very interesting, but their applications have been limited by relatively complex laser configurations, extreme temperature conditions, and additional losses.

In this Letter, we choose an Nd:YVO_4 crystal to build a diode-end-pumped CW dual-wavelength laser running at 1064 and 1066 nm simultaneously, with the consideration of ideal optical and physical characteristics of the Nd:YVO_4 crystal for a multi-wavelength laser operation[14,20,21]. In our experiments, the optimum oscillation condition for the dual-wavelength operation was achieved by tuning the angle between the *c*-axis of Nd:YVO_4 crystal and the polarization direction of the pump light. The maximum output powers at a 2.85 W pump power were 0.55 and 0.54 W at wavelengths of 1064 and 1066 nm, respectively. The linear and short laser cavities brought our dual-wavelength laser obvious advantages of compact configuration and low threshold, which are attractive for practical THz sources based on DFG.

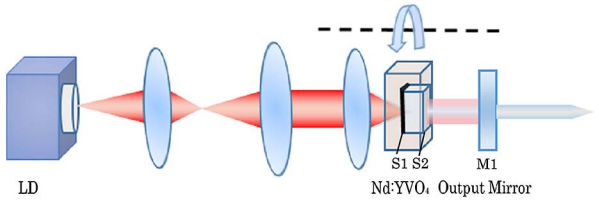

Fig. 1. Experimental setup of CW dual-wavelength Nd:YVO_4 laser.

The experimental setup is shown schematically in Fig. 1. The optical pumping was done by using a high-brightness free-space diode laser that produced horizontally polarized 808 nm pump light. The emitting diode outputted 3.8 W of pump power with an emission bandwidth of 5.0 nm. An optical system made of three achromatic lenses was employed in order to image the pump spot into the Nd:YVO_4 crystal. A conventional a-cut Nd:YVO_4 crystal with dimensions of 4 mm × 4 mm × 3 mm and a doping concentration of 1 at.% was selected as the laser medium, of which one surface (S1) was high reflection (HR) coated with reflectivity $R > 99.8\%$ at 1064 and 1066 nm. The other surface (S2) of the Nd:YVO_4 crystal was antireflection (AR) coated ($R = 0.026\%$ at 1064 and 1066 nm) to reduce the cavity losses for both wavelengths. In order to deal with the excess heat that was generated during pumping, the Nd:YVO_4 crystal was surrounded with tin foil and tightly clamped inside a Cu holder. Its surface temperature was kept at about 15°C by using circulating cold water for active temperature control.

In our experiment, the laser resonator with a linear and compact configuration was used, as shown schematically as Fig. 1. A high-Q cavity was formed by the HR-coated facet (S1) of the Nd:YVO_4 and a curved mirror M1 with a reflectivity about $R = 99.5\%$ at 1064 and 1066 nm. The HR-coated facet (S1) of the Nd:YVO_4 was used as a plane input mirror, and M1 with a radius of curvature 300 mm was used as the output coupler, both of which had a high transmission at 808 nm ($T > 98\%$). The total geometric cavity length (S1–M1) was as short as 10 mm. We used a thin-film optical filter to separate the output wavelength mixing pump laser and then measured the corresponding total output powers of the dual-wavelength laser with a power meter (COHERENT PowerMax PM30). The spectral properties of the output were measured using a spectrometer (Princeton Instruments Action SP2500).

As shown in Fig. 2, we achieved the fundamental emission at 1064 nm when the polarization direction of the pump light is parallel to the crystal's c-axis (identical to the π polarization in Ref. [22]). The 1064 nm laser had a low threshold of 0.15 W and a maximum output power of 1.25 W at a pump power of 3 W. When it grew to over 3 W, the output power showed roll-over behavior as the pump power increased. This can be attributed to the thermal lensing effect in the Nd:YVO_4 crystal[23]. The output spectrum shows that the strongest laser line at 1064 nm is the only one amplified in this case

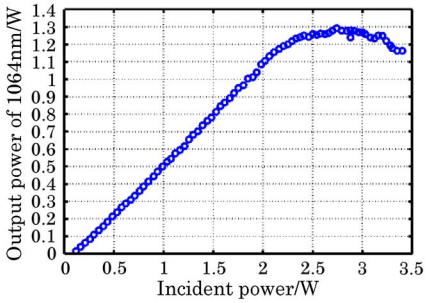

Fig. 2. Output power of 1064 nm laser as a function of the incident pump power.

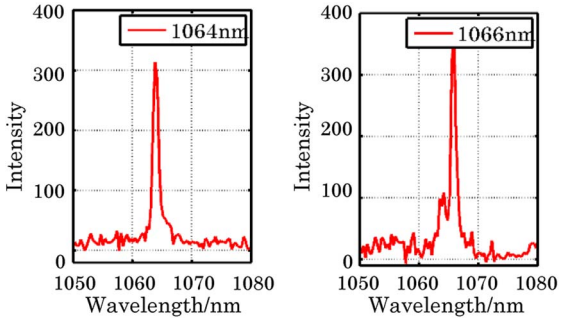

Fig. 3. Output spectrum of the Nd:YVO_4 laser with the pump light polarized parallel to the crystal's c-axis (left) and b-axis (right).

(see Fig. 3). Then, the a-cut Nd:YVO_4 crystal was rotated by 90° around the cavity axis, which is also the lasing direction, making the polarization direction of the pump light parallel to the crystal's b-axis (identical to the σ polarization in Ref. [22]). We observed the laser line at 1066 nm had an intensity that was much stronger than that at 1064 nm, as shown in Fig. 3.

In order to achieve the optimal dual-wavelength operation, we rotated the Nd:YVO_4 crystal around the cavity axis to change the angle between the c-axis of the Nd:YVO_4 crystal and the polarization direction of the pump light, instead of controlling the output mirror tilt angle[24]. The best performances of the CW dual-wavelength laser realized in our experiment are shown in Figs. 4 and 5. The laser was working at 1064

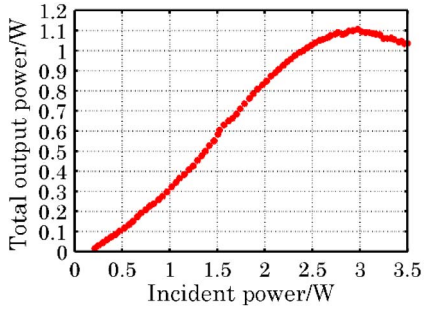

Fig. 4. Total output powers of the dual-wavelength laser at 1064 and 1066 nm as a function of the incident pump power.

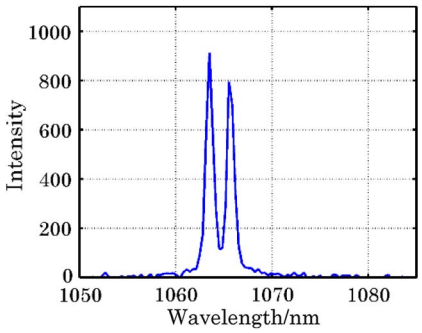

Fig. 5. Output spectrum of the dual-wavelength Nd:YVO_4 laser at the incident pump power of 2.85 W.

and 1066 nm simultaneously with a stable relative intensity. The total dual-wavelength output power as a function of the pump power is shown in Fig. 4. Up to 1.1 W total output power was achieved at the incident pump power of 2.85 W, corresponding to an optical conversion efficiency of 36.7%. At the peak output, the dual-wavelength laser had an optical spectrum, as shown in Fig. 5. From this, we can deduce the relative intensity and then calculate the separate output power for each wavelength. In this way, we obtained the output power of the dual-wavelength Nd:YVO_4 laser as a function of the incident pump power for wavelengths of 1064 and 1066 nm, respectively, according to the measured total output power and the corresponding spectrum at each pump point (see Fig. 6). The two wavelength lasings have similar changing tendencies to the total output power. The threshold pump power was about 0.4 W for both wavelengths. The maximum output powers of 1064 and 1066 nm were 0.549 and 0.541 W at a pump power of 2.85 W, respectively. From the real-time detection of the spectrometer, we can see that slight fluctuations of the relative intensity of 1064 and 1066 nm occur due to the gain competition and the vibrations of the optical platform. For a test interval of 15 min, the fluctuation of the relative intensity was about ±5%.

According to the detailed study of the spectroscopic properties of the Nd:YVO_4 crystal[15,25], the 1064 and 1066 nm lasings come from transitions between energy

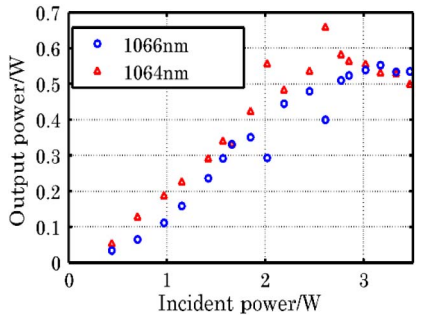

Fig. 6. Output power of the dual-wavelength Nd:YVO_4 laser as a function of the incident pump power for wavelengths of 1064 and 1066 nm.

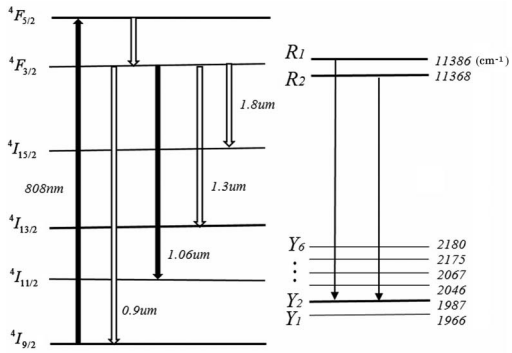

Fig. 7. Transitions within Nd:YVO4 crystal (left) between different energy levels, (right) from energy level $^4F_{3/2}$ to $^4I_{11/2}$ with Stark splitting resulting in 1064 and 1066 nm emissions.

levels with Stark splitting, as shown in Fig. 7. The left side shows the transitions within the Nd:YVO_4 crystal between different energy levels. As long as the appropriate choices and adjustments are made, you can get a very rich laser output. Shen *et al.*[15] revealed that the ratio of the stimulated-emission cross section among the $^4F_{3/2} \rightarrow {}^4I_{9/2}$, $^4F_{3/2} \rightarrow {}^4I_{11/2}$, and $^4F_{3/2} \rightarrow {}^4I_{13/2}$ transitions is a significant factor having influence on multi-wavelength operations in Nd lasers. Among these transitions, $^4F_{3/2} \rightarrow {}^4I_{11/2}$ has a higher fluorescence branching ratio and is the most effective one to generate laser wavelengths in the 1.06 μm band. A further spectroscopic study[25] of this crystal has revealed that there are five or six emission bands within the $^4F_{3/2} \rightarrow {}^4I_{11/2}$ transition resulting from Stark splitting, as shown on the right side of Fig. 7. The 1064 nm radiation comes from the $R_1 \rightarrow Y_2$ transition and the 1066 nm radiation from the $R_2 \rightarrow Y_2$ transition. Normally, laser emissions at 1066 nm cannot compete successfully with other emissions due to their relatively small stimulated emission cross section and their difficulty suppressing parasitical oscillations, as shown in previous work using the traditional method[22].

The breakthrough made by our work is to generate the 1066 nm wavelength simultaneously with 1064 nm from one Nd:YVO_4 laser through good balance of the stimulated emission cross sections for both wavelengths. The Nd:YVO_4 crystal[26] has a tetragonal structure with lattice constants $a = b \neq c$. According to Ref. [22], the pumping condition with respect to the crystal axis has significant influence on the emission spectrum of the Nd:YVO_4 crystal. For the $^4F_{3/2} \rightarrow {}^4I_{11/2}$ transition of Nd^{3+} ions, the most intense emission under π polarization pumping is centered at 1064 nm, and the peak stimulated emission cross section is much greater than the others, as shown in Fig. 8. That is why the laser was running at the single wavelength of 1064 nm when the Nd:YVO_4 crystal used in our laser was set up to make the pump light polarized parallel to the crystal's c-axis. When it comes to σ polarization pumping, the most intense emission is centered at 1066 nm, while the stimulated emission cross

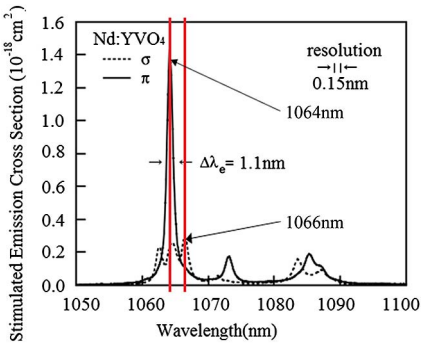

Fig. 8. Effective stimulated emission cross section from $^4F_{3/2}$ to $^4I_{11/2}$ of Nd:YVO_4[22].

sections of the three main peaks between 1060 and 1070 nm have relatively similar values. The distinct anisotropy of the emission property of the Nd:YVO_4 crystal provides an available way to adjust the ratio of the stimulated-emission cross section for the wanted output wavelengths.

In practice, we rotated the Nd:YVO_4 crystal around the cavity axis (see Fig. 1) without any adjustment of the pump light; a small angle existed between the c-axis of the Nd:YVO_4 crystal and the polarization direction of the pump light, as shown in Fig. 9. As a result, the horizontally polarized pump light E is orthogonally decomposed into Ec and Eb along the crystal's c-axis and b-axis, respectively, where the Ec component contributes to the stimulated emission cross section of 1064 nm like the π polarization pumping, and the Eb component contributes to the stimulated emission cross sections of the three main peaks, including 1066 nm, like the σ polarization pumping. Thus, when the Nd:YVO_4 crystal was rotated to adjust the angle between the vector E and the crystal's c-axis, the ratio of Ec to Eb was changed, leading to the good balance of the stimulated emission cross sections for dual-wavelength generation. This is the key for our Nd laser to work at 1064 and 1066 nm simultaneously. Previous works reported that both the stimulated emission cross sections and fluorescence branching ratios determine the output of the mirror reflectivity ratio between the two lasing wavelengths[6]. Usually, when designing the reflectivity of the output mirror, one can select a small reflectivity for a large stimulated emission cross section in the operation of a dual-wavelength laser.

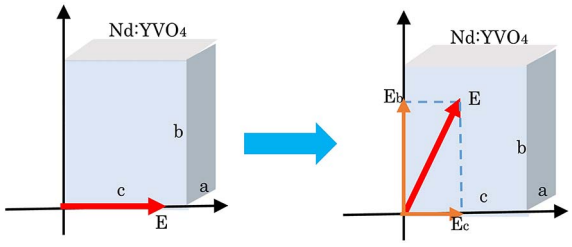

Fig. 9. Relationship between the polarization direction of the pump light E and the Nd:YVO_4 crystal axis.

Reference [27] regulated the dual-wavelength output powers by adjusting the correlation coefficient. In contrast, we do not need to change the output mirror angle or output mirror reflectivity ratio between the two lasing wavelengths in our laser systems. Instead, we just simply changed the angle of laser crystal to get the stable CW dual-wavelength operation without additional optical elements.

In conclusion, a CW dual-wavelength Nd:YVO_4 laser operating at 1064 and 1066 nm is realized. The gain competition within the crystal is regulated by the angle tuning of the laser crystal to change the ratio of stimulated emission cross section for the two wavelengths. At 2.85 W pump power, the maximum output powers at wavelengths of 1064 and 1066 nm are 0.55 and 0.54 W, respectively. The linear resonate cavity is as short as 10 mm, which brings the laser advantages of a miniature configuration and low threshold. Furthermore, we make an attempt to interpret this phenomenon that we can rotate the laser crystal around the pumping and laser directions to control the gain competition within the crystal. We anticipate that such a dual-wavelength laser can be very attractive for the development of compact THz sources based on DFG.

References

1. A. J. Lee and H. M. Pask, Opt. Express **23**, 8687 (2015).
2. L. Gu, Z. Tan, Q. Wu, C. Wang, and J. Cao, Chin. Opt. Lett. **13**, 081402 (2015).
3. A. J. Lee and H. M. Pask, Opt. Lett. **39**, 442 (2014).
4. S. Ge, J. Liu, P. Chen, W. Hu, and Y. Lu, Chin. Opt. Lett. **13**, 120401 (2015).
5. A. J. Lee, Y. He, and H. M. Pask, IEEE J. Quantum Electron. **49**, 357 (2013).
6. Y. F. Chen, Appl. Phys. B **70**, 475 (2000).
7. V. Kubeček, M. Drahokoupil, P. Zátorský, M. Čech, and P. Hiršl, Proc. SPIE **6998**, 69980W (2008).
8. R. P. Mildren, H. M. Pask, H. Ogilvy, and J. A. Piper, Opt. Lett. **30**, 1500 (2005).
9. A. A. Sirotkin, S. V. Garnov, A. I. Zagumennyi, Y. D. Zavartsev, S. A. Kutovoi, V. I. Vlasova, L. Di Labio, W. Lüthy, T. Feurer, and I. A. Shcherbakov, Laser Phys. **19**, 1083 (2009).
10. P. Zhao, S. Ragam, Y. J. Ding, and I. B. Zotova, Opt. Lett. **36**, 4818 (2011).
11. L. J. Chen, S. J. Han, Z. P. Wang, J. Y. Wang, H. J. Zhang, H. H. Yu, S. Han, and X. G. Xu, Appl. Phys. Lett. **102**, 011137 (2013).
12. C. Y. Cho, T. L. Huang, S. M. Wen, Y. J. Huang, K. F. Huang, and Y. F. Chen, Opt. Express **22**, 25318 (2014).
13. A. Brenier, Opt. Lett. **40**, 4496 (2015).
14. Z. Lin, Y. Wang, B. Xu, H. Y. Xu, and Z. P. Cai, Laser Phys. **26**, 015801 (2016).
15. H. Y. Shen, R. R. Zeng, Y. P. Zhou, G. F. Yu, C. H. Huang, Z. D. Zeng, W. J. Zhang, and Q. J. Ye, Appl. Phys. Lett. **56**, 1937 (1990).
16. Y. J. Sun, C. K. Lee, J. L. Xu, Z. J. Zhu, Y. Q. Wang, S. F. Gao, H. P. Xia, Z. Y. You, and C. Y. Tu, Photon. Res. **3**, A97 (2015).
17. B. Wu, P. P. Jiang, D. Z. Yang, T. Chen, J. Kong, and Y. H. Shen, Opt. Epress **17**, 6004 (2009).
18. P. Zhao, S. Ragam, Y. J. Ding, and I. B. Zotova, Opt. Lett. **35**, 3979 (2010).
19. Y. P. Hang, C. Y. Cho, Y. J. Huang, and Y.F. Chen, Opt. Express **20**, 5644 (2012).

20. X. Li, Chin. Opt. Lett. **14**, 021404 (2016)
21. X. Li, A. J. Lee, H. M. Pask, J. A. Piper, and Y. Huo, Opt. Lett. **36**, 1428 (2011).
22. Y. Sato and T. Taira, Jpn. J. Appl. Phys. **41**, 5999 (2002).
23. J. L. Blows, T. Omatsu, J. Dawes, H. Pask, and M. Tateda, IEEE Photonic Tech. Lett. **10**, 1727 (1998).
24. F. Pallas, E. Herault, J. Zhou, J. F. Roux, and G. Vitrant, Appl. Phys. Lett. **99**, 241113 (2011).
25. Y. Sato and T. Taira, IEEE J. Sel. Top. Quantum Electron. **11**, 613 (2005).
26. H. J. Zhang, L. Zhu, X. L. Meng, Z. H. Yang, C. Q. Wang, W. T. Yu, Y. T. Chow, and M. K. Lu, Cryst. Res. Technol. **34**, 1011 (1999).
27. L. J. Chen, Z. P. Wang, S. D. Zhuang, H. H. Yu, Y. G. Zhao, L. Guo, and X. G. Xu, Opt. Lett. **36**, 2554 (2011).